

A Surfactant-based Method for Carbon Coating of $\text{LiNi}_{0.8}\text{Co}_{0.15}\text{Al}_{0.05}\text{O}_2$ Cathode in Li Ion Batteries

Youngmin Chung, Seong-Hyeon Ryu, Jeong-Hun Ju, Yu-Rim Bak, Moon-Jin Hwang, Ki-Won Kim,[†]
Kwon-Koo Cho,[†] and Kwang-Sun Ryu*

*Department of Chemistry, University of Ulsan, Ulsan 680-749, Korea. *E-mail: ryuks@ulsan.ac.kr*

[†]i-Cube Center, ITRC for Energy Storage and Conversion, Gyeong Sung National University, Jinju 660-701, Korea

Received April 8, 2010, Accepted June 22, 2010

A $\text{LiNi}_{0.8}\text{Co}_{0.15}\text{Al}_{0.05}\text{O}_2$ (LNCAO/C) active material composite cathode was coated with carbon. The conductive carbon coating was obtained by addition of surfactant during synthesis. The addition of surfactant led to the formation of an amorphous carbon coating layer on the pristine LNCAO surface. The layer of carbon coating was clearly detected by FE-TEM analysis. In electrochemical performance, although the LNCAO/C showed similar capacity at low C-rate conditions, the rate capability was improved by the form of the carbon coating at high current discharge state. After 40 cycles of charge-discharge processes, the capacity retention of LNCAO/C was better than that of LNCAO. The carbon coating is effectively protected the surface structure of the pristine LNCAO during Li insertion-extraction.

Key Words: Lithium-ion battery, Cathode, Carbon-coating, Lithium-nickel-cobalt-aluminum oxide, Surfactant

Introduction

In recent years, lithium-ion batteries have become an alternative power source for various portable electronic devices, such as mobile phones, laptop computers, and electric vehicles. This versatile usage is due to the high energy density of lithium-ion batteries compared with other rechargeable batteries.

The electrode material commonly used in present day commercial lithium-ion batteries is LiCoO_2 .¹ However, only 50% of the theoretical capacity of LiCoO_2 (~140 mAh/g) can be effectively utilized in the voltage range of 3 ~ 4.25 V.² Many authors have investigated LiCoO_2 structure and reactivity towards electrolytes. Based on their studies, increase or decrease in the capacity fading of a LiCoO_2 cathode was achieved by substituting metal ions for cobalt, or through surface modifications with chemically more stable or inert materials. $\text{LiNi}_{0.8}\text{Co}_{0.2}\text{O}_2$ is a very promising cathode material, with a high capacity and a mid-range cost, as compared to other lithium-ion batteries.^{3,4} When nickel was doped for cobalt in LiCoO_2 , 65% of the theoretical capacity was achieved. Many studies have suggested that the surface modifications of LiCoO_2 and $\text{LiNi}_{0.8}\text{Co}_{0.2}\text{O}_2$ electrodes with a metal oxide (Al_2O_3 , TiO_2 and ZrO_2) will lead to better capacity retention than uncoated LiCoO_2 or $\text{LiNi}_{0.8}\text{Co}_{0.2}\text{O}_2$, when the cell is cycled above 4.2 V.⁵⁻⁸ In $\text{LiNi}_{0.8}\text{Co}_{0.15}\text{Al}_{0.05}\text{O}_2$ (LNCAO), there is partial Al cation substitution for nickel and cobalt.⁹ The effects of Al doping were attributed to the suppression of phase transition or lattice changes during cycling,¹⁰ as well as to the suppression of the decomposition reaction between the electrode and electrolytes.

In the present study, we report a simple and effective method for the preparation of carbon-coated LNCAO cathode materials. Many studies have indicated that the surface coating approach is an effective method to improve thermal and structural stability, as well as to increase the cycling ability.¹¹ The carbon coating method improves the electrochemical properties of the cathode. Other synthesis methods for carbon coating have also been

used, such as a solid state reaction with a carbon-containing precursor, and carbon coating by the deposition of a carbon thin film. In this study, the carbon source was a surfactant that was in good contact with the metal oxide surface. The synthesis was a self-assembled monolayer (SAM) process. In a SAM process, materials such as metals, metal oxides, semi-conductors, or glasses are used as substrates, and alkylsiloxane monolayers, fatty acids, or alkanethiolate monolayers are used as surface-active materials. When the substrates were in a solution of surface-active materials, chemisorptions occurred between the substrates and the surface-active head groups.¹² The binding energies of the chemisorptions were on the order of tens of kcal/mol (40 ~ 45 kcal/mol for thiolate on gold). When the surfactant was added into an LNCAO dispersed solution, the surfactant could directly attach to the surface of the LNCAO particles. When the precursor was heated in the air, carbon-coated LNCAO was obtained. The cycling behavior of carbon-coated LNCAO cathodes was evaluated, resulting in C-rates between 4.3 or 4.5 ~ 2.8 V. The effect of carbon coating on the structural and electrochemical properties was investigated in detail for the LNCAO/C composite.

Experimental

Pristine LNCAO powder (Ecopro Co. Ltd., Korea) was used as an electrode. To prepare a carbon-coated LNCAO sample, the LNCAO powder was dispersed in distilled water and sonicated for 20 minutes using a Branson 3200 ultrasonic liquid processor operating at 200 kHz. The sodium dodecyl sulfate (SDS: surfactant, Aldrich, 0.5 wt %) was slowly added to the coating solution and the solution was sonicated for 1h, resulting in uniform slurry. The SDS used as a carbon source was sintered with LNCAO. The powder composite was vacuum dried at 80 °C for 10 h. After drying, the powder was calcined in air at 600 °C for 5 h.

To investigate the LNCAO or LNCAO/C crystal structural,

we analyzed the prepared powder by X-ray diffraction (XRD). XRD patterns were measured with a Rigaku ultra-X (Cu K_{α} radiation, 40 kV, 120 mA) at a step scan rate of $0.02^{\circ}/\text{s}$ in the $20 \sim 80^{\circ}$ 2θ range. The morphologies and sizes of the powder particles were measured by scanning electron microscopy (FE-SEM; Supra 40) analysis and field emission transmission electron microscopy (FE-TEM; JEM 2100F, JEOL).

The 2016R coin cells were assembled with LNCAO or LNCAO/C, super-p, and polyvinylidene fluoride (PVDF; KF #1300) in *N*-methyl pyrrolidinone (NMP; Aldrich) at a mass ratio of 92:4:4 ($0.008 \text{ g}/\text{cm}^2$) in an argon-filled glove box. The LNCAO or LNCAO/C cathode, Li metal anode, and a separator (Cellgard 2500), were mixed for making the positive electrode. The 1.3 M LiPF_6 (Technosemichem Co. LTD, Korea) in a 3:3:4 (vol. ratio) mixture of ethylene carbonate (EC), dimethyl carbonate (DMC), and ethylene methyl carbonate (EMC) was used as electrolyte solution. The cells were galvanostatically tested (Maccor) for charge and discharge cycling with current densities of $0.1 \sim 3 \text{ C}$ (each 5 cycles) and for 40 cycles (0.1 C) in the range of $2.8 \sim 4.3 \text{ V}$ or 4.5 V , to evaluate the electrochemical behavior of the cathode materials. Cyclic voltammetry (CV, Macpile Biology) was conducted at a $0.05 \text{ mV}/\text{sec}$ scan rate and $2.7 \sim 4.8 \text{ V}$. For differential scanning calorimetry (DSC) experiments, the cells were fully charged to 4.3 V and immediately opened in the Ar-filled dry box. The remaining excess electrolyte on the electrode was removed and inserted into the gold plate stainless steel sample pan. The thermal scan was performed with DSC (Shimadzu DSC-60) at scan rate of $10^{\circ}\text{C min}^{-1}$ from 50°C to 400°C .

Results and Discussion

The LNCAO/C composite was prepared by chemical adsorption of surfactant within the mixed oxide layer, (Fig. 1) using a SAM synthesis process. SDS was the surfactant used as surface-active material. The ultrasound treatment appeared to be more effective than magnetic stirring for the SDS dispersion on the LNCAO surface. Because of strong adsorbate-adsorbent interactions between the LNCAO and SDS, the SDS monolayer was arrayed on the LNCAO surface. SDS maintained its arrangement when water was removed from the solution, because of the carbon chain intermolecular interactions. SDS carbon chains formed the carbon layer on the LNCAO surface.

Structure analysis. Figure 2 shows the X-ray diffraction (XRD) patterns of pristine LNCAO and the LNCAO/C composite. The XRD patterns are indexed as a layered α - NaFeO_2 type structure, assuming a hexagonal geometry in the $R\bar{3}m$ space group. The XRD pattern of LNCAO/C had an identical structural group to LNCAO, with no site disordering. The SDS were formed a thin layer as amorphous monolayer. There was no difference between the coated and uncoated particles except small shift of peak position. The average thickness of the surface carbon layer of LNCAO/C was estimated using the Scherrer's equation calculation.¹³

$$D = K\lambda / \beta \cos \theta$$

D is the average diameter of the crystals (in angstroms), λ is the X-ray wave length ($\lambda = 1.5406 \text{ \AA}$), and K is the shape factor

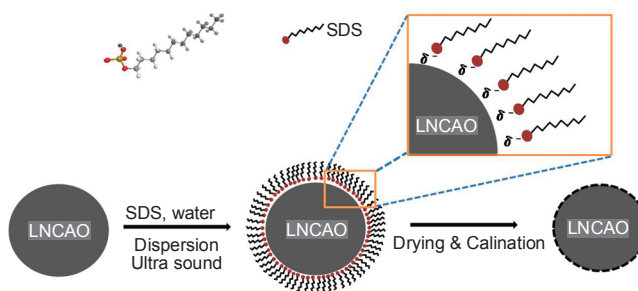


Figure 1. The preparation scheme of the LNCAO/C composite with surfactant.

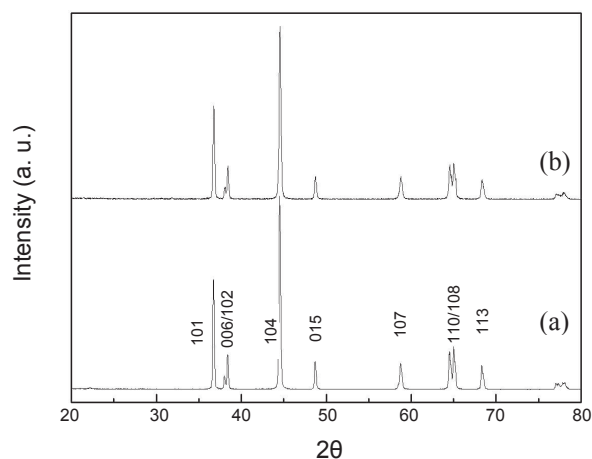


Figure 2. XRD patterns of (a) pristine LNCAO and (b) LNCAO/C.

($K = 0.9$). The value of K depends on several factors, including the Miller index of the reflecting plane and the shape of the crystals.^{14,15} θ is Bragg angle (in degrees). We compared with the 110 or 108 peaks of LNCAO and LNCAO/C. β is the full width at half-maximum of 110 or 108 peaks. The difference of the average diameter for LNCAO and LNCAO/C was calculated above equation. From these results, the carbon coating thickness was estimated to be $2.5 \sim 3 \text{ nm}$. Therefore, we thought that the SDS was formed a thin layer and amorphous monolayer.

Morphology. Figure 3 shows the field emission scanning electron microscopy (FE-SEM) images of the pristine LNCAO and the LNCAO/C composite. The pristine LNCAO (Fig. 3 (a)) samples, which look like $8 \sim 12 \mu\text{m}$ spheres, were comprised of smooth-edged $0.2 \sim 0.5 \mu\text{m}$ polyhedral particles. The FE-SEM images of LNCAO/C (Fig. 3 (b)) did not show any morphological changes, because of the thin layer of carbon coating.

Figure 4 shows the field emission transmission electron microscopy (FE-TEM) images of the pristine LNCAO and the LNCAO/C composites. TEM analysis was used to investigate in detail the shapes of the particles and their surface morphologies. The pristine LNCAO had the smooth and clear surface and no other coating layer as like Fig. 4 (a). Fig. 4 (b) clearly showed a distinguishable carbon coating layer existing around the surface of the pristine LNCAO. A $2 \sim 3 \text{ nm}$ thick amorphous carbon-coating layer was seen on the carbon phase-grown composite. In the XRD analysis, the thickness of the layer was determined to be $2.5 \sim 3 \text{ nm}$ using Scherrer's equation.

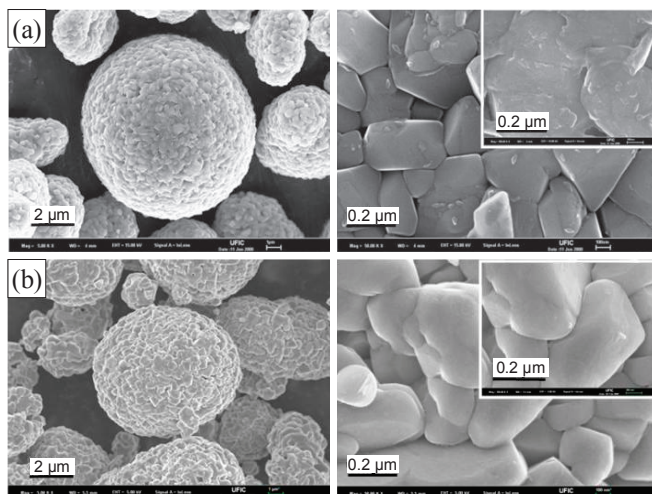


Figure 3. FE-SEM images of (a) pristine LNCAO and (b) LNCAO/C.

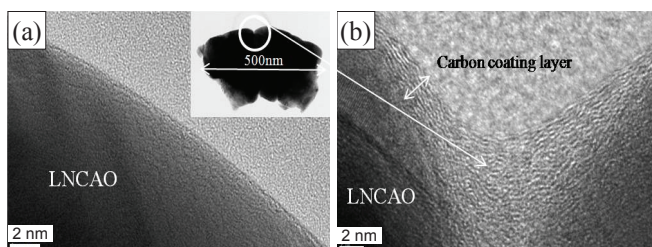


Figure 4. FE-TEM images of (a) pristine LNCAO and (b) LNCAO/C.

Electrochemical performance.

Cyclic voltammetry: Cyclic voltammetry (CV) is sensitive to the phase transformations of materials during electrochemical reactions. A slow scan CV was performed to examine the effect of the coating on the phase transition that accompanies the charge-discharge process.¹⁶ There are three peaks in the CV curve of LiNiO_2 because there are multiple phase transitions during the CV scan. The deintercalation and intercalation processes occurred between 2.7 ~ 4.8 V, at a constant current density of 0.5 mV/sec. The deintercalation currents seen in the CV were larger than the intercalation currents, which agrees with the first cycle charge and discharge capacities for each material. The large irreversible first cycle capacities of the materials are reflected in the cyclic voltammograms. Figure 5 compares the cyclic voltammograms of the pristine LNCAO and the LNCAO/C composite. The peaks due to the phase transitions appear at 3.70, 4.01, and 4.21 V, representing the phase transitions of the hexagonal phase (H1) to the monoclinic (M) phase at the first peak, the M phase to the second hexagonal phase (H2) at the second peak, and the H2 to a third hexagonal phase (H3) at the third peak.¹⁷ The CV curve from the pristine LNCAO (Fig. 5 (a)) exhibits three transitions during oxidation, indicating the presence of four different phases. There is no significant difference in peak degradation between LNCAO and LNCAO/C, indicating that the carbon coating does not affect the pristine LNCAO redox intercalation.

Discharge capacity and cyclic performance: Rate capability is one of the important electrochemical characteristics of a lithium secondary battery being used in power storage applica-

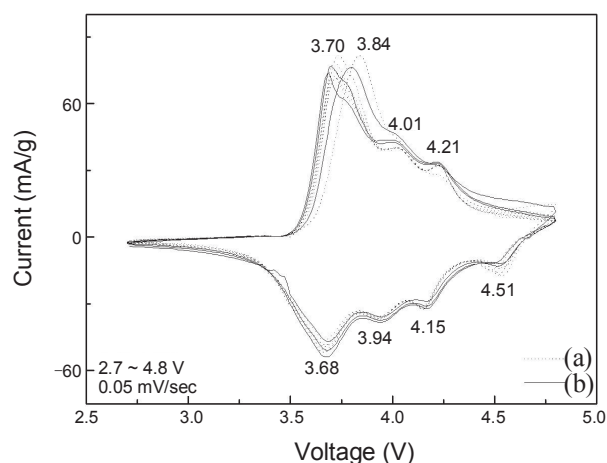


Figure 5. Cyclic voltammograms of (a) pristine LNCAO and (b) LNCAO/C with a voltage range of 2.7 - 4.8 V at 0.05 mV/sec.

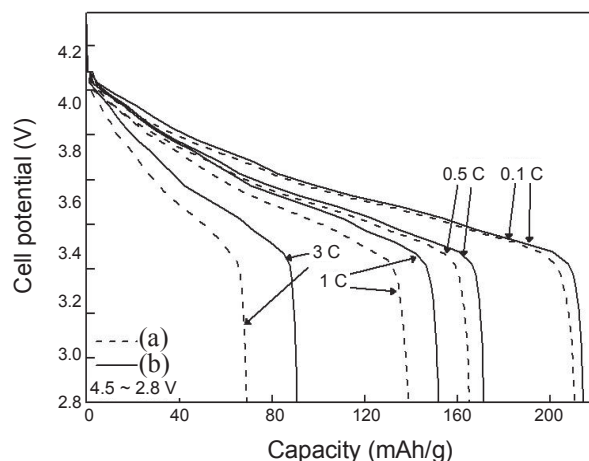
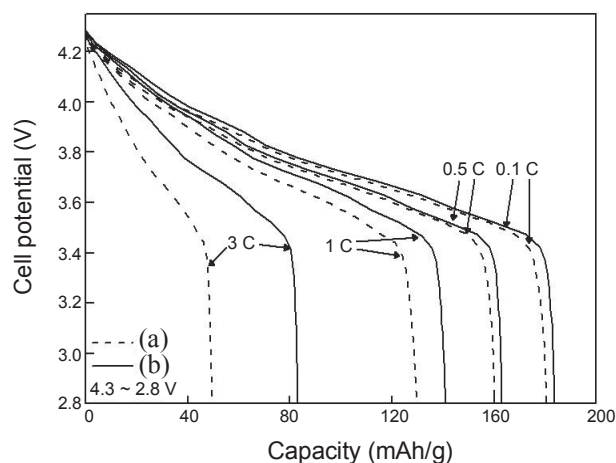


Figure 6. Discharge capacities (a) pristine LNCAO and (b) LNCAO/C with a voltage range of 4.3 or 4.5 - 2.8 V at 0.1, 0.5, 1, and 3 C.

tions. In the present study, rate capability is investigated at different C-rates (current densities). For each 5 cycle average, the charge and discharge process are performed at the same C-rate: between 4.3 or 4.5 ~ 2.8 V at room temperature. At 4.3 ~ 2.8 V (Fig. 6 (a)), LNCAO/C had discharge capacities of 183, 165, 140,

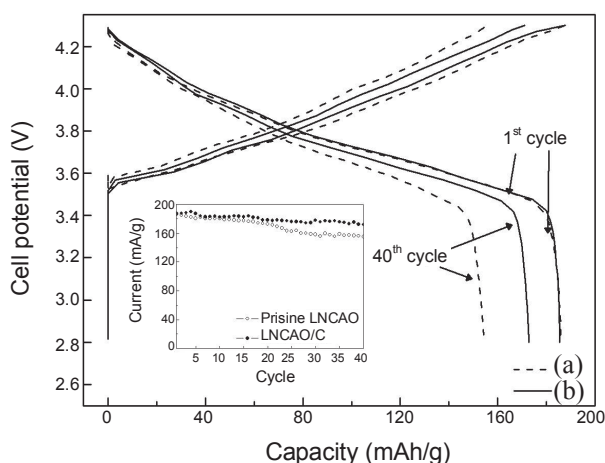


Figure 7. Charge-discharge capacities vs. cycle number of (a) pristine LNCAO and (b) LNCAO/C for 40 cycles at 0.1 C.

and 83 mAh/g at 0.1, 0.5, 1, and 3C, respectively. Meanwhile, the pristine LNCAO had discharge capacities of 181, 160, 128, and 46 mAh/g. It is noticeable that a much lower over potential was observed in the LNCAO/C than in the pristine LNCAO, especially at high C-rates, indicating that the carbon coating significantly reduced the polarization of the cathode/electrolyte interface in the cell. The reduction of cell polarization was probably due to the improvement in conductivity of the compound. At 4.5 ~ 2.8 V (Fig. 6 (b)), the LNCAO/C cathode had a higher discharge capacity at every C-rate than did the pristine LNCAO. Furthermore, at high C-rates, there was a larger variation in discharge capacities. After carbon coating, at high C-rates, the stability of the structure may be increased during the discharge.

Figure 7 presents the charge and discharge profiles of the pristine LNCAO and the LNCAO/C cathode materials after the 1st and 40th cycles, respectively, in the cut-off voltage 4.3 ~ 2.8 V at 0.1 C. The initial discharge capacity of the pristine LNCAO was 181 mAh/g, and the LNCAO/C electrodes delivered an initial discharge capacity of 182 mAh/g, maintaining excellent cycling behavior with little capacity loss after 40th cycles (172 mAh/g). The capacity retention of the carbon-coated LNCAO/C (~ 93%) was also better than that of the pristine LNCAO (~ 86%). The carbon coating stabilized the structure during the Li insertion-extraction. The carbon coating was correlated with improved structural stability of the cathode and better capacity retention during the cycling. Thus, carbon coating on LNCAO/C leads to better electrochemical performance of the electrode.

Thermal stability: The thermal stability of cathode materials, especially in a highly de-lithiated state, is important for their practical application. Figure 8 presents DSC data of the pristine LNCAO and the LNCAO/C composite electrode, which was charged to 4.3 V and used same quantity of electrolyte solution. The electrode using the pristine LNCAO showed a large exothermic peak (640 J/g) at 248 °C with an onset of deposition near 200 °C. The thermal stability of the LNCAO/C, on the other hand, was improved with an onset of deposition near 220 °C. The heat of exothermic peak is 360 J/g at 261 °C, which was significantly smaller than that for the pristine LNCAO. The improved

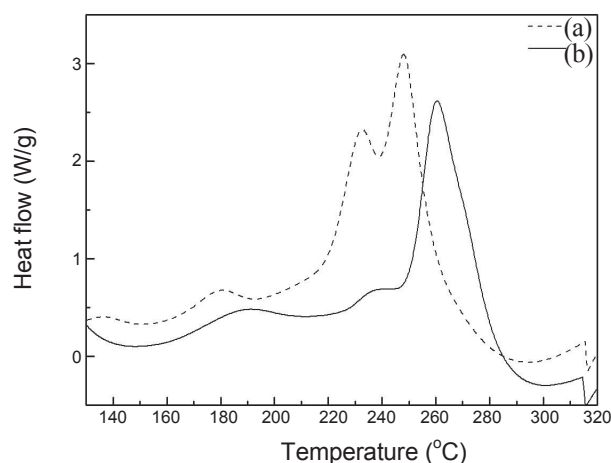


Figure 8. Differential scanning calorimetry (DSC) curve of (a) pristine LNCAO and (b) LNCAO/C electrodes, which are charged to 4.3 V.

thermal stability of the LNCAO/C can be attributed to a thin carbon coating layer, which plays a protective role in preventing the cathode particles from being attacked by HF in the electrolyte solution and hence suppresses the release of oxygen from the host lattice.¹⁸

Conclusions

The carbon coating of the LNCAO surface was done with a surfactant (SDS), using chemical adsorption SAM synthesis techniques. The FE-TEM analysis showed that the surfactant made a 2 ~ 3 nm thick amorphous carbon coating layer on surface of the pristine LNCAO. By evaluating the electrochemical performance of LNCAO and LNCAO/C, we concluded that the carbon coating effectively prevented the degradation of electrochemical performance at high currents. The reduction of the cell polarization of cathode/electrolyte interface was probably due to the improvement in conductivity of the compound. The discharge capacity and the capacity retention of the LNCAO/C were induced by the carbon coating, which effectively acted on the surface stability of electrode material during insertion-extraction of Li ion. The improved electrochemical performance was attributed to the thin carbon coating layer, which supported the highly de-lithiated cathode from direct contact with the liquid electrolyte. Thermal stability at a highly charged state of the LNCAO/C was slightly improved. The thin carbon coating layer played a role of preventing the cathode particles from being attacked by HF in the electrolyte solution and hence suppressed the release of oxygen from the host lattice.

Acknowledgments. This work was supported by Mid-career NRF grant funded by Researcher Program through MEST (No. 2009-0083818).

References

- Nagaura, T.; Taza, K. *Prog. Batt. Sol. Cells* **1990**, *9*, 20.
- Zou, M.; Yoshio, M.; Gopukumar, S.; Yamaki, J. *Chem. Mater.* **2002**, *15*, 1310.
- Chen, Z.; Dahn, J. R. *Electrochem. Solid-State Lett.* **2003**, *6*, 221.

4. Kannan, A. M.; Rabenberg, L.; Manthiram, A. *Electrochem. Solid-State Lett.* **2003**, *6*, 16.
 5. Liu, H.; Zhang, Z.; Gong, Z.; Yang, Y. *Solid State Ionics* **2004**, *166* (3-4), 317.
 6. Wang, Z.; Wu, C.; Liu, L.; Wu, F.; Chen, L.; Huang, X. *J. Electrochem. Soc.* **2002**, *149*(4), 466.
 7. Cho, J.; Kim, Y. J.; Kim, T. J.; Park, B. *Angew. Chem. Int. Ed.* **2001**, *40*(18), 3367.
 8. Cho, J.; Lee, J. G.; Kim, B.; Park, B. *Chem. Mater.* **2003**, *15*, 3190.
 9. Cho, J. *Chem. Mater.* **2000**, *12*, 3089.
 10. Lee, K. K.; Kim, K. B. *J. Electrochem. Soc.* **2000**, *147*(5), 1709.
 11. Ryu, K. S.; Lee, S. H.; Koo, B. K.; Lee, J. W.; Kim, K. M.; Park, Y. *J. J. Appl. Electrochem.* **2008**, *38*, 1385-1390.
 12. Nuzzo, R. G.; Allara D. L. *J. Am. Chem. Soc.* **1983**, *105*, 4481.
 13. Klöng, H. P.; Alexander, L. E. *X-ray Diffraction Procedures for Crystalline and Amorphous Materials* **1954**.
 14. Pouget, J. P.; Jozefowicz, M. F.; Epstein, A. J.; Tang, X.; MacDiarmid, A. G. *Macromolecules* **1991**, *24*, 779.
 15. Moon, Y. B.; Cao, Y.; Smith, P.; Heeger, A. J. *Polym Commun.* **1991**, *30*, 196.
 16. Kavan, L.; Gratzel, M. *Electrochem. Solid-State Lett.* **2002**, *5*, A39.
 17. Li, W.; Reimers, J. N.; Dahn, J. R. *Solid State Ionics* **1993**, *67*, 123.
 18. Sun, Y. K.; Cho, S. W.; Lee, S. W.; Yoon, C. S.; Amine, K. *J. Electrochem. Soc.* **2007**, *154*, A168.
-